RSC Advances

PAPER

View Article Online
View Journal | View Issue

Cite this: *RSC Adv.*, 2023, **13**, 27624

Healable supramolecular micelle/nano-encapsulated metal composite phase change material for thermal energy storage

Adem Ali Muhabie *

Phase change materials (PCMs) have emerged as promising materials for latent heat storage due to their characteristic solid–liquid phase transition behavior during the melting and cooling process. Among them, organic phase change materials are commonly used in latent heat storage. Herein, new phase change self-assembled micelles (PCSM) demonstrated thermal-based phase transition properties. Silver nanoparticles were employed as an additive to improve the thermal properties of the shape-stabilized composite PCSM. The surface morphology and microstructure, general thermal properties and heat adsorption and release behaviors of the samples were characterized with the aid of TEM, SEM, OM, DSC, TGA and DLS techniques. The DSC curve showed that the latent heat adsorption and temperature, heat capacity and thermal reliability of the composite PCSM improved upon the addition of Ag NPs. The TGA curves demonstrated that the presence of Ag NPs increased the onset decomposition temperature and the peak weight loss temperature. PCSM demonstrated low thermal conductivity, whereas the composite PCSM showed better thermal conductivity. This study provides new insight into the promising preparation of healable composite PCMs and their application in thermal energy storage.

Received 1st June 2023
Accepted 25th August 2023

DOI: 10.1039/d3ra03673a

rsc.li/rsc-advances

1. Introduction

Phase change materials (PCMs) have attracted considerable attention in the field of energy storage/release due to their diverse potential applications such as heat transfer media,[1] intelligent buildings,[2] and energy storage technologies.[3] This is because PCMs have desirable characteristics including suitable melting temperatures, negligible supercooling through phase change, outstanding phase transition behavior, high heat storage capacity and non-toxicity.[4,5] PCMs are categorized as organic PCMs and inorganic PCMs, regardless of their chemical structure. Organic PCMs mainly include higher fatty acids, paraffin, polyolefin, and polyethylene glycol, which have advantages compared to inorganic PCMs including minor corrosion, less prone to phase separation and good fixed molding.[6] However, the utilization of organic PCMs for thermal energy storage has several drawbacks due to their thermal instability, low latent heat per unit mass, supercooling, low thermal conductivity, and seepage during solid–liquid phase transition,[7] which hinder their practical applications. In this case, fixing organic PCMs in spherical nanomaterials to synthesize shape-stable phase change materials is an effective way to solve the above-mentioned problems. To achieve the best shape-stable phase change materials, it is usually important to prepare composite phase change materials by mixing pure PCMs with additive chemicals, which enhance the strength and eliminate the drawbacks of PCM. One of the factors affecting the thermal performance of latent heat storage systems is the low thermal conductivity of most PCMs.[8] The low thermal conductivity of PCMs results in materials having low heat charge and discharge efficiency during melting and solidification processes. Thus, to overcome the above-mentioned limitations, organic PCMs are often mixed with thermal conductivity enhancers or packed into a thermally conductive matrix.[9] Accordingly, improving the heat exchange rate performance of PCMs is a crucial parameter in terms of efficiency and economy. A typical and significant behavior of PCMs is the change in their physical state from solid to liquid and *vice versa* during the melting and solidification process without a chemical change. Leakage from the liquid state of PCMs also has a major impact on their practical application. Thus, PCMs are protected by dispersing them in materials that block the seepage process from the polymer network structure, protecting against the excessive heat that attacks the PCM.[10] In addition, additives are also used as shape-forming and thermal stabilizers of phase change materials. There are many possible strategies to improve the heat storage performance, thermal stability and reliability, heat density and conductivity of phase transition properties,[11] and prevent the leakage of PCMs such as increasing their surface area, dispersing high-conductive additives and fabrication of micro-sized and nano-sized PCM composites.[12] A wide variety of additives has been dispersed in PCMs to improve their thermal properties, such as metals

Woldia University, Faculty of Natural and Computational Sciences, Department of Chemistry, Woldia, Ethiopia. E-mail: alimohabe2003@gmail.com

(nickel, copper, and silver),[13,14] alloys,[15] metal oxides (CuO and SiO_2),[13,16] carbon-based 2D materials,[17,18] and ceramic materials (BN, WSe_2 and MoS_2).[19–21] Additives are receiving attention for the fabrication of composite PCMs for energy storage technology due to their unique characteristics such as large specific surface area, diverse applications, and stable structure. In thermal energy storage systems, additives will increase the thermal conductivity but slightly reduce the latent heat during the melting and cooling cycle because they are not involved in the phase change reversibility. Hence, researchers have been working on balancing the thermal conductivity and latent heat of composites. Metallic particles including copper, silver, aluminum and nickel have been widely studied for improving the heat storage of PCMs as result of their high thermal conductivity. It has been reported that incorporating paraffin into metallic fibers provides an improvement in the heat transfer and effective thermal conductivity of the PCM composite with an insignificant reduction in its latent heat capacity.[22] Copper nanoparticles with a size of 20 nm were blended in paraffin wax to prepared PCM composites. It was found that the addition of Cu increased the thermal conductivity of paraffin. Cu NPs were also used as a nucleation agent to decrease the supercooling process in the phase transition. Porous composite PCMs containing copper and nickel exhibited increased thermal conductivity compared to PCMs.[23]

Composite PCMs can be prepared *via* various method such as phase inversion-assisted vacuum impregnation and solution encapsulation method. Furthermore, composite phase change materials can self-assembly into shape-stable solid–liquid phase reversible materials *via* impregnation under vacuum at 100 °C for 15 min to eliminate bubbles and excess moisture contained in samples. Impregnation is also employed to incorporate PCMs in other supporting materials. For example, copper oxide microparticles served as a filler to improve the shape-stability and thermal performance of composite PCMs, which were prepared *via* simple vacuum impregnation. Wang *et al.* incorporated copper fibers in paraffin to improve the heat energy transfer efficiency of a PCM and reported that the thermal conductivity of the PCM composite was better without a large decrease in latent heat capacity. Silver metal was applied as a thermal stability additive in composite PCMs, greatly increasing the thermal transfer and thermal properties such as reliability, stability and shape-forming ability of the composite materials.[22,24] Moreover, silver is commonly considered a biocompatible nanoparticle in human and animals. The addition of silver can not only improve the thermal stability, biocorrosion, cooling, conductivity, and resistance of composite phase change materials but also minimize the instability or aggregation of nanomaterials during the DSC heating/cooling thermal cycle.[25] In the preparation of composite organic PCMs, due to the high contact surface area of additives and high capillary, they can transfer heat to the absorbent of PCMs very well, and thus avoid liquid leakage.[23,26] Therefore, due to the properties of silver, it is selected as an additive dispersed in PCMs to improve the thermal properties of the composite. Then, silver nanoparticles are synthesized *via* an *in situ* reduction strategy and encapsulated *via* phase change self-assembled micelles (APPG).

In this study, phase change self-assembled micelles (PCSM) were synthesized using adenine and polypropylene glycol diacrylate (PPGDA) through a Michael addition reaction. Phase change self-assembled micelle difunctional oligomers containing nucleobases can hierarchically self-assemble in water into nanosized spherical micelles and enable controlled drug carrier and release, bio imaging, and cellular uptake, and thus used in chemotherapeutic application *in vitro*. These supramolecular phase change materials possess excellent properties such as non-corrosiveness, biocompatibility, non-toxicity, hydrophilicity, and degradability. However, to the best of our knowledge, there is no report on the chemical structure, surface morphology, thermal-based phase transition behavior, thermal properties, latent heat adsorption and releasing properties of phase change supramolecular micelle and silver nanoparticle composites. CPCSM (APPG/Ag) was prepared using silver nanoparticles as the core material and hierarchal-layered PCSM as the shell or carrier to further improve the thermal/shape stability and thermal conductivity of CPCSMs. The structure and morphology change (FTIR, OM, SEM, DLS, and HRTEM), solid–liquid phase reversibility properties and latent heat storage parameters (DSC, TD-FTIR) of the supramolecular phase change material composites were explored and analyzed in detail. The excellent thermal stability, phase change properties, thermal reliability and thermal conductivity were attributed to the addition of silver nanoparticles to PCSMs, forming regenerated hierarchal-layered microsphere micelles. The latent heat of crystallization, crystallization temperature, latent heat of melting, melting temperature, degradation temperature, heat capacity, super cooling properties and thermal state reversibility properties were studied during changes in the material from the solid state to the liquid state. Based on the obtained results, the composite PCSMs have wide application in thermal energy storage and thermal management systems.

2. Experimental

2.1. Preparation of phase change self-assembled micelles (PCSMs)

The new phase change self-assembled micelles, which were denoted as adenine bifunctional polypropylene glycol (A-PPG), were synthesized using adenine and polypropylene glycol diacrylate (PPGDA) by slightly modifying the synthesis procedure described in the previous work.[27] APPG was self-assembled in into nanosized spherical micelles *via* hydrogen bonding attraction force between the adenine moieties.

2.2. Preparation of composite phase change self-assembled micelles (CPCSMS)

The composite phase change material was prepared using the phase change self-assembled micelles and silver nitrate *via* a solution encapsulation method. A solution of A-PPG was prepared by dissolving dried A-PPG in tetrahydrofuran, then silver nitrate was added and the mixture was sonicated for 3 h at

25 °C and poured onto glass plates to form pristine powder. Subsequently, the powder was heated in an oven for 12 h to eliminate volatile impurities and solvent. The synthetic route is shown in Fig. 1.

2.3. Characterization methods

Fourier transform infrared (TD-FTIR) spectroscopy measurements were performed using a PerkinElmer Spectrum Two system (PerkinElmer, Buckinghamshire, U.K.) in the wavenumber range of 4000–600 cm^{-1}. High-resolution tunneling electron microscopy (HRTER), field emission scanning electron microscopy (FE-SEM) and optical microscopy (OM) were performed to analyze the size, microstructure and morphology of the phase change materials. Differential light scattering measurement was conducted to determine the size of the spherical micelle phase change materials. A Q-20 DSC instrument (New Castle, DE, USA) was used to study the latent heat, phase transition behavior, and latent heat temperature. Test samples (*ca.* 10 mg) were weighed and sealed in an aluminum sample pan and scanned in the temperature range of −70 °C to 130 °C at a heating and cooling rate of 10 °C min^{-1}. Accelerated thermal cycling testing was conducted in a high-low temperature chamber to evaluate the thermal reliability of the phase change materials. The tests were conducted for 100 consecutive heating/cooling scan cycles at a heating rate of 10 °C min^{-1}. A TGA Q500 thermogravimetric analyzer (Q500-0743TGA) was used to the test thermal stability and decomposition resistance of the samples. A platinum pan was loaded with *ca.* 5 mg of sample material and heated from room temperature to 900 °C at a ramp rate of 10 °C min^{-1} under a nitrogen atmosphere. The weight loss was recorded as a function of temperature. The thermal conductivity of the samples was analyzed using a thermal conductivity meter. Particle size and particle size distribution were determined directly using a Nano Brook 90Plus PALS (Brookhaven Instruments Corp., Holtsville, NY, USA).

3. Results and discussion

Microscopy methods were applied to characterize the morphology and microstructure of PCSM and CPSCM. The high-resolution OM image in Fig. 2a shows the morphological surface of CPCSM, which has a microcapsule like structure. The microcapsules possessed a hierarchical-layered spherical shape

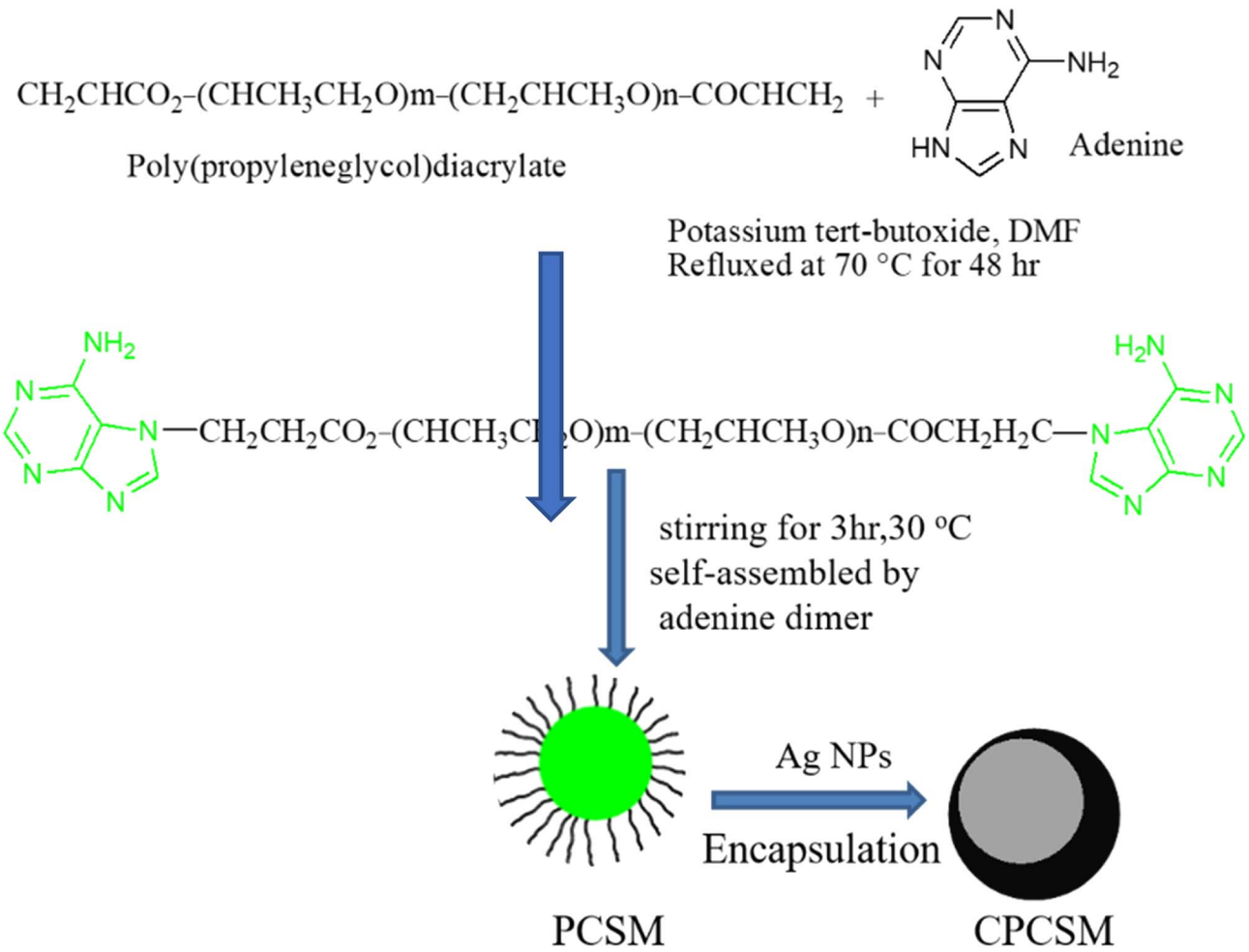

Fig. 1 Procedure for the preparation of CPCSM.

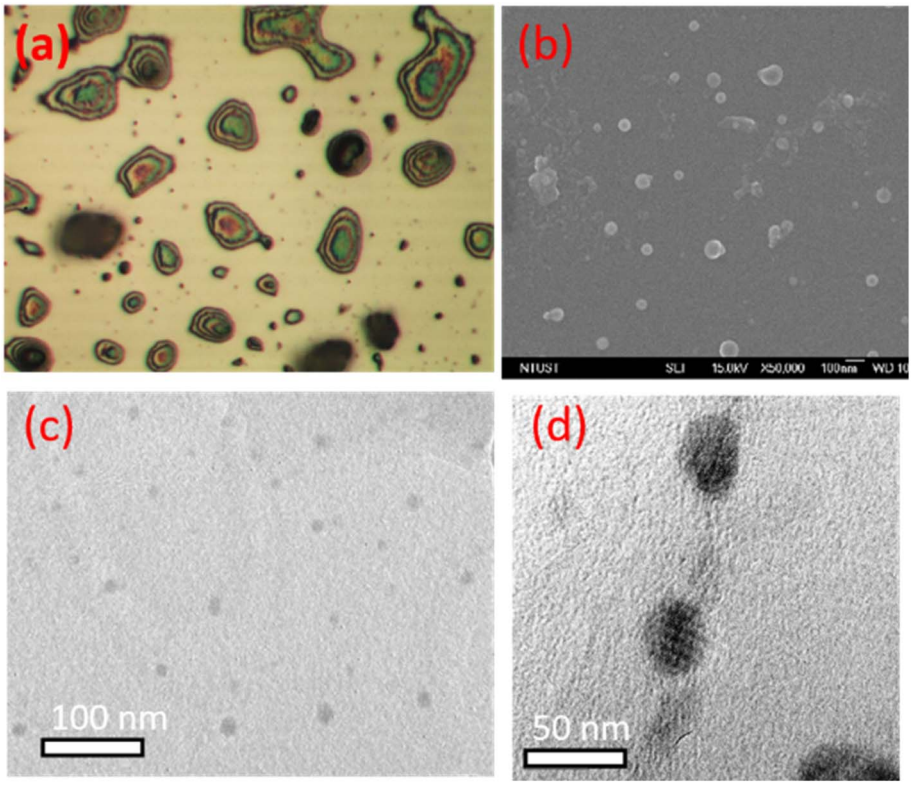

Fig. 2 Optical microscopy image (a) and SEM image (b) of PCSM. HRTEM image of Ag nanoparticles (c) and composite PCSM (d).

with a size in the range of 115.32 nm to 205.98 nm, which is consistent with the DLS results (Fig. 2).

Fig. 2b obviously shows a self-assembled spherical micelle morphology on the silicon wafer and the size of the PCSM micelles was determined by measuring the diameter of the micelles. The measured size of the micelles was found to be in the range of 56 nm to 95 nm, which is consistent with the TEM results. The synthesized polymer containing nucleobases was responsible for the spontaneous self-assembly into nanosized spherical micelles, which are applicable for nanoparticle encapsulation, bio imaging, controlled drug delivery and thermal energy storage. The possible strategy for the formation of micelles is intramolecular hydrogen bonding between nucleobases.[28] The HR-TEM image in Fig. 2c shows the appearance of spherical Ag nanoparticles, which are uniformly deposited on the substrate and the size of the metallic filler is in the range of 10.34 nm to 18.01 nm. As shown in the HR-TEM image in Fig. 2d, the composite PCSM nanomaterial formed from Ag NPs and phase change supramolecular polymer possessed a spherical morphology (Fig. 1). The black circle region indicates the decomposed organic framework of the composite. The PCSM nanomaterial encapsulated the metallic filler and its diameter increased. The microcapsule encapsulated the silver nanoparticles, and the encapsulation efficiency was 82.65%. This further implies that the A-PPG chains tended to form layer-by-layer micro- and nano-sized materials through the intermolecular hydrogen bonds between adenine moieties.[29] The polymeric chain, pendant group of the adenine ring system, amine, imine, and carbonyl reaction-responsible groups have the tendency to encapsulate silver by electrostatic interaction, oxidation/reduction, or electron transfer reaction mechanism.[27] The synthesized nanosized micelles demonstrated phase transition behavior towards small temperature changes, making them useful for heat energy storage applications. The micelles were formed by dimerization, and then the self-assembly of APPG *via* intermolecular hydrogen forces.[30]

Further, differential light scattering (DLS) measurement was conducted to realize the size of the samples in aqueous solution at different concentrations. The size distribution for 2.5 mg mL^{-1} aqueous solution of synthesized pure nanomaterial is shown in Fig. 3a, where the size of the PCSM micelles at the concentration of 1.5 mg mL^{-1}, 2.5 mg mL^{-1}, and 5.0 mg mL^{-1} are 135.12 nm, 160.67 nm and 182 nm, respectively. Fig. 2b shows that most of the CPCSM nanoparticles have a dimeter of 135 nm at 2.5 mg mL^{-1}. The size measured with FE-SEM and TEM was somewhat smaller than that from DL, which may be due to the dehydration of water from the micelles as result of drying or spin coating sample on the silicon wafer.

Differential scanning calorimetry (DSC) was used to characterize the thermal properties of PCSM and CPCMs such as phase reversibility, supercoiling degree, specific heat capacity, latent heat, and phase transition temperatures of heat flow in the materials.

The DSC curves of the samples and the corresponding detailed latent heat and thermal properties are revealed in Fig. 3 and Table 1, respectively. PCSM exhibited a sharp melting and

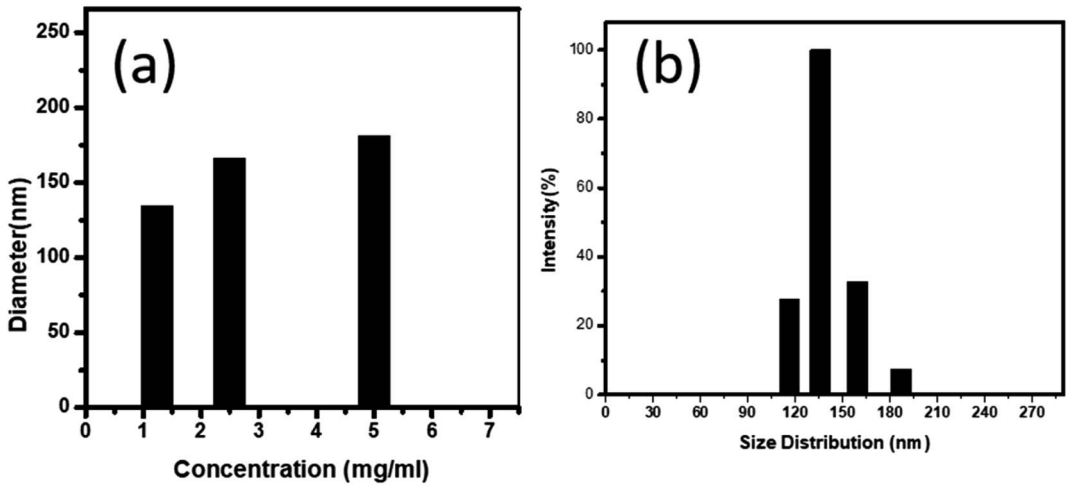

Fig. 3 (a) Size of PCSM at different concentrations and (b) size distribution of PCSM as a function of intensity.

solidification peak with strong intensity, as shown in Fig. 4a and b, respectively. The heat of enthalpy is one of the crucial factors of PCSMs to store heat energy of endothermic and exothermic equilibrium reaction, which is established during melting and freezing of PCSMs as a critical indicator their phase transition reversibility behavior. The onset melting temperature (T_{mo}), peak melting temperature (T_{pm}), and final melting temperature (T_{mf}) during DSC heat flow of melting PCSM were 87.80 °C, 110.47 °C, 119.75 °C, respectively. The onset crystallization temperature (T_{co}), peak crystallization temperature (T_{pc}), and final crystallization temperature (T_{cf}) during the DSC cooling scan of pure PCSM are 61.76 °C, 46.85 °C, and 38.88 °C, respectively. The latent heat of melting (ΔH_m) and crystallization (ΔH_c) are 254.07 J g^{-1} and 235 J g^{-1}, respectively, indicating that pure PCSM is an excellent phase change nanomaterial with outstanding phase change reversible properties in the temperature range of −70 °C to 110.47 °C. The composite PCSM and PCSM revealed almost similar thermal properties when heat was charged and discharged during the phase transition process, as shown in the DSC curve in Fig. 4b. It was found that the melting and solidifying temperature peaks of CPCSMs and DSC thermal properties of PCSM are consistent with the previous results.[31] However, composite PCSMs revealed broader and shorter endothermic and exothermic bands compared to PCSM. In addition, the peaks slightly shifted to the left for PCSM and its thermal temperatures were slightly reduced, which is attributed to the addition of silver, mechanically reinforcing and thermally stabilizing the synthesized materials.[32] Fig. 4c shows the thermal phase reversibility properties of PCSM in aqueous solution. It was found that after heating at 60 °C, the PCSM aqueous solution exhibited a cloudy or opaque appearance, indicating that PCSM has phase transition behavior and thermal stimuli behavior to different environments (temperature, pH, and light).[33] The phase change reversibility of PCSM occurred due to the hydrogen bond dissociation and reconstruction between adenine–adenine interactions.[27] During heating, the disintegration of the numerous hydrogen bonds and the dissociation of the hydrogen bond interaction between the carbonyl groups and adenine moieties are responsible for the physical state change

Table 1 Thermal properties of PCSM and CPCSM according to the DSC heat flow curves[a]

Sample, subscript scan number	Melting latent heat (ΔH_m) and temperatures (°C)				Solidification latent heat (ΔH_s) and temperatures (°C)				Supercooling
	T_{om}	T_{pm}	T_{fm}	ΔH_m	T_{os}	T_{ps}	T_{fs}	ΔH_s	ΔT
$PCSM_1$	88.67	114.0	116.27	254.07	61.76	46.85	38.88	−235.60	68.67
$PCSM_2$	88.80	110.47	119.75	252.07	61.76	46.65	38.58	−175.60	63.62
$PCSM_{50}$	88.79	98.98	105.4	234.07	55.85	46.85	38.97	−229.25	52.13
$PCSM_{100}$	88.12	98.67	105.02	233.85	55.68	46.23	38.45	−224.56	51.32
$PCSM_{500}$	79.57	98.09	104.43	232.36	55.24	46.15	38.21	−224.38	51.18
CPCSM1	68.80	110.47	119.75	233.95	60.37	45.82	37.50	−189.68	87.80
$CPCSM_2$	68.67	104.95	116.27	233.65	58.37	45.2	38.50	−169.68	52.28
$CPCSM_{50}$	68.56	98.32	104.3	230.65	54.12	45.21	38.44	−126.78	50.11
$CPCSM_{100}$	68.43	98.09	103.88	229.64	53.78	45.34	38.12	−125.98	49.33
$CPCSM_{500}$	68.13	89.87	103.58	229.62	53.68	45.25	38.10	−125.90	49.23

[a] T_{om}: onset melting temperature, T_{pm}: melting peak temperature, T_{fm}: final melting temperature, T_{os}: onset solidification temperature, T_{ps}: solidification peak temperature, and T_{fs}: final solidification temperature of DSC curve.

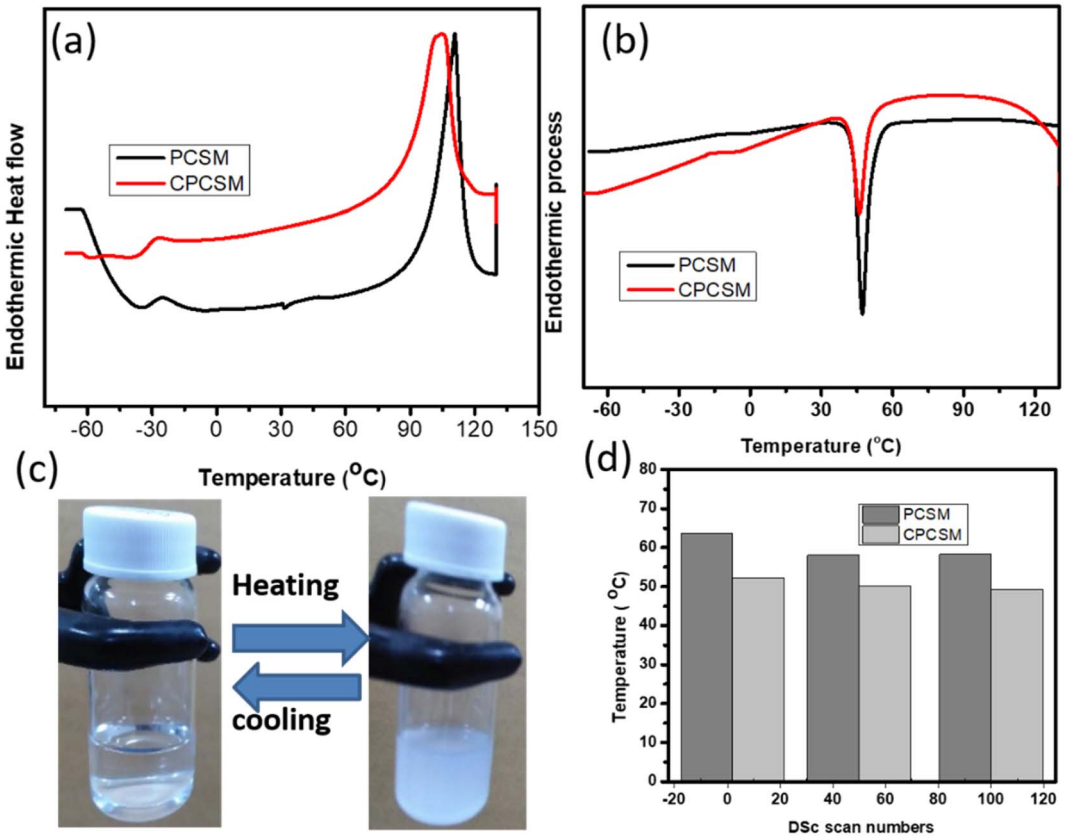

Fig. 4 DSC first heating (a) and first cooling curves (b) for PCSM and CPCSMs. (c) Thermal phase reversibility properties of PCSM in aqueous solution. (d) Supercoiling degree of samples at different DSC scan numbers.

of the solid into a liquid.[34] During the recrystallization process, solidified PCSMs and CPCSMs were formed as a result of hydrogen bond formation and cross-linking or/and non-covalent bond formation.[35]

Supercooling is one of the limitations of PCMs, which should be minimized for the practical application of the synthesized CPCSM. The degree of supercooling of PCSM and CPCSM is shown in Fig. 4d. The supercoiling degree of the composite PCSM was lower than PCSM during the melting/solidification process. Blending of the filler with the supramolecular polymer PCM resulted in a reduction in supercooling and facilitated the heat absorption and release process.

Thermal reliability refers to the latent heat storage performance of phase change materials after multiple melting and cooling processes. It is critical for the synthesized composite phase change self-assembled micelles to have excellent thermal reliability. Thus, to confirm the thermal reliability of the samples, it was important to test them by 500 DSC melting/solidification scans, as shown in Fig. 5a and b. The thermal properties are also shown in Table 1. With an increase in the number of melting-solidification scans by hundreds for PCSM and CPCSM, the phase transition temperatures of the two samples did not significantly differ. Also, their latent heat flow such as melting (ΔH_m) and solidification (ΔH_s) did not significantly change and the thermal reliability results are similar to the previously reported results,[36] indicating that the synthesized samples exhibited an excellent heat charging and discharging performance. This is attributed to the excellent physical hydrogen bond dissociation and reconstruction between the adenine moieties in the equilibrium process.[37] Overall, thermal cycling tests are cost effective and save time because they provide evidence for the thermal consistency and reliability of the samples over the long run, even before their use in a specific application.

Thermal stability is a critical information parameter, which is used to specify the thermal resistance of materials to thermal degradation in the application temperature range. Fig. 5c and d display the TGA curve of PCSM and CPCSM with an increase in temperature from 0 °C to 900 °C under a nitrogen atmosphere and the degradation temperatures are shown in Table 2. Single step degradations were observed for the all samples, where the weight loss is mainly due to the decomposition, and then volatilization of the organic matter. The initial weight loss temperature (T_{in}), weight loss bent temperature (T_{bn}), maximum weight loss temperature (T_{max}), and 96.69% weight loss temperature ($T_{96.69}$) of the composite PCSM were 216.49 °C, 245.33 °C, 349.73 °C and 400 °C, respectively. These degradation temperatures of the composite PCSM were higher than that of PCSM and almost the same as that in previous works.[38] In addition, the TGA curve slightly shifted to the right as the temperature increased as result of the incorporation of silver metal in the PCSM, which improved the thermal stability of the

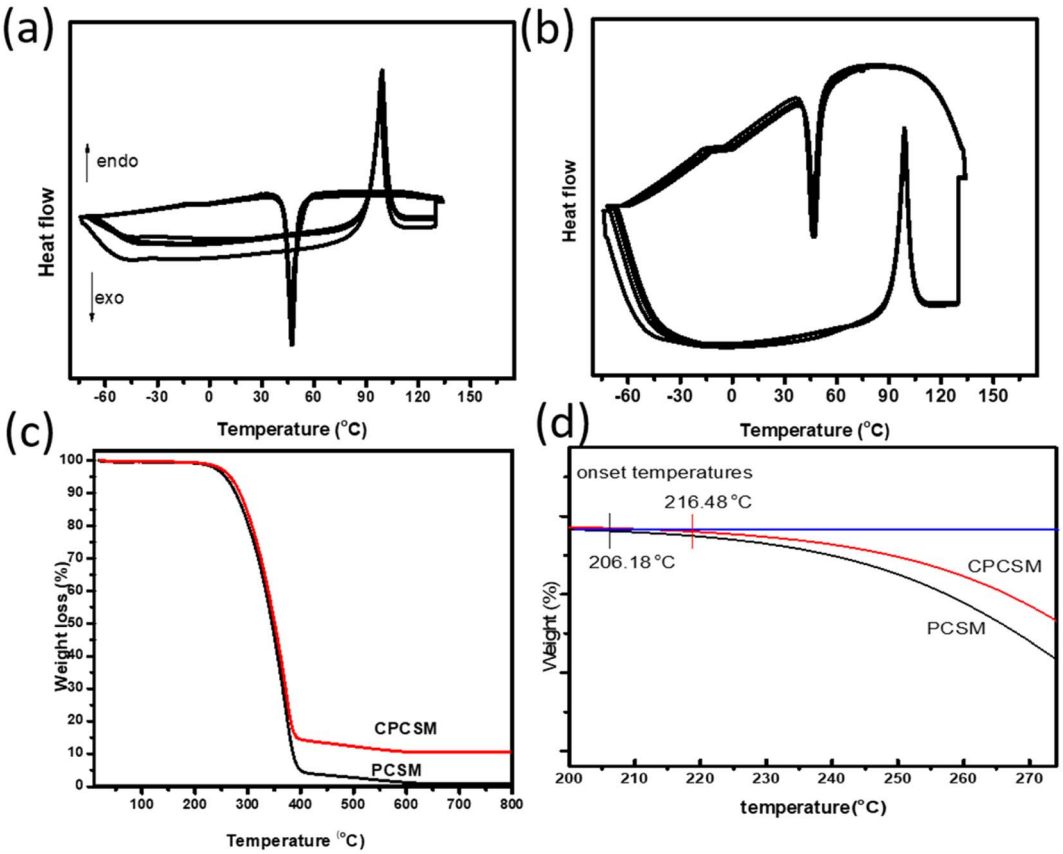

Fig. 5 500 DSC melting/solidification cycles of PCSM (a) and CPCSMs (b). (c) TGA curves of PCSM and CPCSMs and (d) enlarged view of TGA curves in (c).

Table 2 TGA thermal properties of PCSM and CPCSM

Samples	T_{ini} (°C)	T_{bn} (°C)	T_{max} (°C)	$T_{-96.69\%}$ (°C)
PCSM	206.18	241.35	344.74	399.50
CPCSM	216.49	245.33	349.73	400.00

phase change material by protecting the surface of the polymer and delayed its decomposition due to additional protection.[39]

The CPCSM composite exhibited good thermal stability below an application temperature of 250 °C. Moreover, only 4.41 wt% unknown residue was left in PCSM and the residual mass of CPCSM was 14.64 wt%, suggesting loading led to an increase in the thermal stability of the composite due to the higher thermal stability of the fillers in the composite.[40]

The reversible hydrogen bond dissociation and reconstruction during melting and solidification, indicating a physical liquid–solid phase transition, for CPCSM was studied by a TD-FTIR experiment to support the DSC results, as shown in Fig. 6. The peak in the FTIR spectrum of CPCSM changed depending on the heating and cooling temperature. For instance, a new broad peak was observed at 3490 cm^{-1}, indicating the presence of 'free' amine functional groups. During melting at a temperature of 98.5 °C, 105.25 °C and 110 °C, the hydrogen bonding disappeared and new peaks together with band broadening were observed. These new broad peaks are attributed to the dissociation of the hydrogen bond of the adenine dimers.

At room temperature or after the solidification temperature, the free amine peak disappeared in the spectra. At the

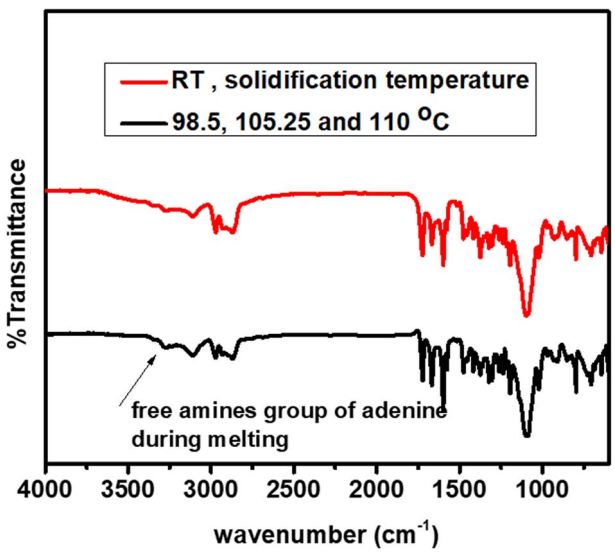

Fig. 6 TD-FTIR spectra of CPCSM at various temperatures.

Table 3 Comparison of the latent heat of melting of PCM between this study and previous studies

Composite phase change materials	ΔH_m (J g^{-1})	Ref
Nanofibrillated cellulose/polydopamine hybrid aerogels	250.4	23
Octadecane and gallium with expanded graphite as a carrier	215.00	22
LDPE/hexadecane/SEBS composite PCMs with the addition of copper oxide	169.74	13
Ionic cross-linked polyvinyl alcohol tunes vitrification and cold-crystallization of sugar alcohol	232.8	30
Paraffin wax phase change materials	150–200	24
Salt hydrate phase change materials	150–250	28
Crosslinked polyurethane/lauric acid composites	118.3	37
Healable supramolecular micelle/nano-encapsulated metal phase change composite material for thermal energy storage	254.07	This work

solidification temperature, the same spectra were obtained as the scan at room temperature due to the reconstruction of the hydrogen bond network or disappearance of the amine functional groups. At the solidification temperature, the self-assembled PCM should present a supramolecular formation in the form of a spherical structure due to the dimerization of the adenine moieties *via* hydrogen bond interactions, π–π stacking between dimers and formation of hydrogen bonds between the ester carbonyl oxygen and adenine moieties. The TD-FTIR results show that the dissociation and reconstruction of the hydrogen bonds between the adenine–adenine moieties and adenine-carbonyl oxygen (NH···O=C) interactions in CPCSM played a great role in the phase change enthalpy (ΔH), phase change temperature and thermal energy storage capacity. The peaks observed at 3284 cm^{-1}, 1715 cm^{-1}, 1668 cm^{-1} and 1598 cm^{-1} are correspond to hydrogen bonded amine (NH) groups, C=O, C–N and C=N stretching vibrations of the adenine fragments, respectively. Obviously, these vibrations are features of the crystallized adenine units in CPCSM. The Ag nanoparticles did not influence the reversible process of hydrogen bonds during the phase change and improved the structural and thermal stability of the CPCSM material. In addition, the large interfacial contact area and strong interface between nanoparticles and the PCSM may help to enhance the phase transition behavior of CPCSM. The homogeneously dispersed composite with outstanding thermal phase reversibility properties and the hydrogen bonding interactions between the adenine chains collectively contributed to the phase transition behavior. Thus, the temperature-dependent phase transition behavior of CPCSM make it highly promising for potential applications in latent heat energy utilization devices.

The metallic filler improved the heat capacity and thermal conductivity of PCSM. The heat capacity is one of the key parameters used to describe the thermal energy storage during a sensible heat process.[41] The heat capacity of PCSM and CPCSM was determine based on their DSC heat-flow curves. The heat capacity of PCSM and CPCSM was 1.02 J g^{-1} °C and 2.31 J g^{-1} °C, respectively. The thermal conductivity of PCSM and CPCSM was 0.19 W m K^{-1} and 0.36 W m K^{-1}, respectively, which is consistent with the results in previous studies.[42] These results show that the heat capacity and thermal conductivity of the samples increased with the addition of silver metal as the filler because the heat transfer by Ag is higher than that by PCSM. In addition, the thermal conductivity of silver is much larger, which has a significant influence on the heat capacity and thermal conductivity of the composites. Given that silver was embedded and encapsulated in the self-assembled spherical nanomaterial, it enhanced the thermal conductivity and energy storage density of PCSM. Nickel could improve the thermal conductivity and heat capacity/density in previous studies on organic PCMs.[43] The present thermal properties of the prepared phase change material composite PCSM are comparable with that in previous reports, as shown in Table 3. Ag NPs increased the thermal energy transfer property and enhanced the heat capacity absorption of the composite PCSMs simultaneously.[44] Therefore, in the prepared CPCSMs, the assembled Ag/APPG composites have potential for use in effective heat energy storage devices and thermal management applications.

4. Conclusion

The fabrication of supramolecular phase change materials with superior thermal properties and high latent heat is critical for the utilization of thermal energy storage. In this study, we designed a simple method to synthesize new supramolecular self-assemble micelles/Ag phase change composites. TEM, SEM, OM, DSC, DLS and TGA were employed to study the compositional, morphological and thermal energy storage properties of PCSM and CPCSMs. The melting temperature, enthalpy of melting, phase transition behavior, crystallization temperature, enthalpy of crystallization, thermal reliability and thermal stability were also measured to evaluate the phase change properties and latent heat storage properties of the samples. The heat charge/discharge during the heating and cooling process were attributed to the formation and dissociation of a hydrogen bond network in the adenine dimerized micelles due to the phase change enthalpy of PCSM upon changing from a solid to liquid, respectively. The thermal properties of CPCSMs improved as result of the incorporation of Ag NPs in PCSM, suggesting their promising characteristics for latent heat energy utilization applications.

Data availability

All the data are included in this article.

Conflicts of interest

The author declare no conflict of interest.

Acknowledgements

I thank Woldia University for the financial support.

References

1 M. M. Umair, Y. Zhang, K. Iqbal, S. Zhang and B. Tang, Novel strategies and supporting materials applied to shape-stabilize organic phase change materials for thermal energy storage–a review, *Appl. Energy*, 2019, **235**, 846–873.

2 S. S. Magendran, F. S. A. Khan, N. Mubarak, M. Vaka, R. Walvekar, M. Khalid, E. Abdullah, S. Nizamuddin and R. R. Karri, Synthesis of organic phase change materials (PCM) for energy storage applications: a review, *Nano-Struct. Nano-Objects*, 2019, **20**, 100399.

3 G. Duttaluru, P. Singh, A. K. Ansu, R. kumar Sharma and S. Mishra, Methods to enhance the thermal properties of organic phase change materials: a review, *Mater. Today: Proc.*, 2022, 685–691.

4 H. Yi, L. Xia and S. Song, Three-dimensional montmorillonite/Ag nanowire aerogel supported stearic acid as composite phase change materials for superior solar-thermal energy harvesting and storage, *Compos. Sci. Technol.*, 2022, **217**, 109121.

5 B. E. Jebasingh and A. V. Arasu, A detailed review on heat transfer rate, supercooling, thermal stability and reliability of nanoparticle dispersed organic phase change material for low-temperature applications, *Mater. Today Energy*, 2020, **16**, 100408.

6 P. Liu, X. Gu, L. Bian, X. Cheng, L. Peng and H. He, Thermal properties and enhanced thermal conductivity of capric acid/diatomite/carbon nanotube composites as form-stable phase change materials for thermal energy storage, *ACS Omega*, 2019, **4**(2), 2964–2972.

7 D. Feng, Y. Feng, P. Li, Y. Zang, C. Wang and X. Zhang, Modified mesoporous silica filled with PEG as a shape-stabilized phase change materials for improved thermal energy storage performance, *Microporous Mesoporous Mater.*, 2020, **292**, 109756.

8 Y. Li, Y. Li, X. Huang, H. Zheng, G. Lu, Z. Xi and G. Wang, Graphene-CoO/PEG composite phase change materials with enhanced solar-to-thermal energy conversion and storage capacity, *Compos. Sci. Technol.*, 2020, **195**, 108197.

9 Y. Grosu, Y. Zhao, A. Giacomello, S. Meloni, J.-L. Dauvergne, A. Nikulin, E. Palomo, Y. Ding and A. Faik, Hierarchical macro-nanoporous metals for leakage-free high-thermal conductivity shape-stabilized phase change materials, *Applied Energy*, 2020, **269**, 115088.

10 W. Yang, R. Lin, X. Li, C. Li, Y. Wu, G. Zhang, X. Liu, S. Li and Y. Wang, High thermal conductive and anti-leakage composite phase change material with halloysite nanotube for battery thermal management system, *J. Energy Storage*, 2023, **66**, 107372.

11 K. Archana, N. G. Pillai, S. S. KV, P. K. Chauhan, R. Sujith, K. Y. Rhee and A. Asif, Enhanced isosteric heat of adsorption and gravimetric storage density of hydrogen in GNP incorporated Cu based core–shell metal–organic framework, *Int. J. Hydrogen Energy*, 2020, **45**(58), 33818–33831.

12 F. Zhong, C. Chen, D. Zhang, R. Yang, X. Huang, K. Yang, H. Qin and X. Yang, A Novel Dendritic Polyaniline/Phytate@ Cu Organic–Metal composite Flame Retardant for Improving Thermal Protection of Epoxy Coatings, *Colloids Surf., A*, 2023, 131635.

13 A. Trigui, M. Abdelmouleh and C. Boudaya, Performance enhancement of a thermal energy storage system using shape-stabilized LDPE/hexadecane/SEBS composite PCMs by copper oxide addition, *RSC Adv.*, 2022, **12**(34), 21990–22003.

14 K. Chen, J. Ding, W. Wang and J. Lu, Shape-stable Bi–Sn–In alloy/Ag/copper foam composite phase change material for thermal storage and management, *Chem. Eng. J.*, 2023, **454**, 140087.

15 T. Kawaguchi, H. Sakai, N. Sheng, A. Kurniawan and T. Nomura, Microencapsulation of Zn–Al alloy as a new phase change material for middle-high-temperature thermal energy storage applications, *Applied Energy*, 2020, **276**, 115487.

16 J. Li, L. He, T. Liu, X. Cao and H. Zhu, Preparation and characterization of PEG/SiO_2 composites as shape-stabilized phase change materials for thermal energy storage, *Sol. Energy Mater. Sol. Cells*, 2013, **118**, 48–53.

17 H. Liu, X. Wang and D. Wu, Fabrication of graphene/TiO_2/paraffin composite phase change materials for enhancement of solar energy efficiency in photocatalysis and latent heat storage, *ACS Sustain. Chem. Eng.*, 2017, **5**(6), 4906–4915.

18 W. Jin, L. Jiang, L. Chen, Y. Gu, M. Guo, L. Han, X. Ben, H. Yuan and Z. Lin, Preparation and characterization of capric–stearic acid/montmorillonite/graphene composite phase change material for thermal energy storage in buildings, *Constr. Build. Mater.*, 2021, **301**, 124102.

19 W. Lee, J. Hong, J. Song, W. Yang and J. Kim, Fabrication of high-performance thermally conductive phase change material composites with porous ceramic filler network for efficient thermal management, *Compos. Sci. Technol.*, 2023, 110092.

20 N. Sun and Z. Xiao, Synthesis and performances of phase change materials microcapsules with a polymer/BN/TiO_2 hybrid shell for thermal energy storage, *Energy Fuels*, 2017, **31**(9), 10186–10195.

21 Y. Cao, D. Fan, S. Lin, F. T. Ng and Q. Pan, Branched alkylated polynorbornene and 3D flower-like MoS_2 nanospheres reinforced phase change composites with high thermal energy storage capacity and photothermal conversion efficiency, *Renewable Energy*, 2021, **179**, 687–695.

22 S. Drissi, T.-C. Ling and K. H. Mo, Thermal efficiency and durability performances of paraffinic phase change materials with enhanced thermal conductivity–a review, *Thermochim. Acta*, 2019, **673**, 198–210.

23 H. Zhang, L. Wang, S. Xi, H. Xie and W. Yu, 3D porous copper foam-based shape-stabilized composite phase change materials for high photothermal conversion, thermal conductivity and storage, *Renewable Energy*, 2021, **175**, 307–317.

24 J. Ji, Y. Wang, X. Lin, B. Liu and X. Zhang, Fabrication of highly thermal conductive and shape-stabilized phase change materials, *J. Energy Storage*, 2021, **44**, 103256.

25 W. Luo, X. Hu, Y. Che, S. Zu, Q. Li, X. Jiang and D. Liu, Form-stable phase change materials enhanced photothermic conversion and thermal conductivity by Ag-expanded graphite, *J. Energy Storage*, 2022, **52**, 105060.

26 L. Zhang, Z. Shi, B. Zhang and J. Huang, Silver attached graphene-based aerogel composite phase change material and the enhancement of thermal conductivity, *Materials*, 2020, **13**(15), 3271.

27 C.-C. Cheng, A. A. Muhabie, S.-Y. Huang, C.-Y. Wu, B. T. Gebeyehu, A.-W. Lee, J.-Y. Lai and D.-J. Lee, Dual stimuli-responsive supramolecular boron nitride with tunable physical properties for controlled drug delivery, *Nanoscale*, 2019, **11**(21), 10393–10401.

28 A. A. Muhabie, C.-H. Ho, B. T. Gebeyehu, S.-Y. Huang, C.-W. Chiu, J.-Y. Lai, D.-J. Lee and C.-C. Cheng, Dynamic tungsten diselenide nanomaterials: supramolecular assembly-induced structural transition over exfoliated two-dimensional nanosheets, *Chem. Sci.*, 2018, **9**(24), 5452–5460.

29 D. G. Atinafu, W. Dong, U. Berardi and S. Kim, Phase change materials stabilized by porous metal supramolecular gels: gelation effect on loading capacity and thermal performance, *Chem. Eng. J.*, 2020, **394**, 124806.

30 Y. Cao, Y. Meng, Y. Jiang, S. Qian, D. Fan, X. Zhou, Y. Qian, S. Lin, T. Qian and Q. Pan, Healable supramolecular phase change polymers for thermal energy harvesting and storage, *Chem. Eng. J.*, 2022, **433**, 134549.

31 Y. Yao, Y. Cui and Z. Deng, Phase change composites of octadecane and gallium with expanded graphite as a carrier, *RSC Adv.*, 2022, **12**(27), 17217–17227.

32 Y. Tan, X. Du, Z. Du, H. Wang and X. Cheng, Form-stable phase change composites based on nanofibrillated cellulose/polydopamine hybrid aerogels with extremely high energy storage density and improved photothermal conversion efficiency, *RSC Adv.*, 2021, **11**(10), 5712–5721.

33 B. T. Gebeyehu, A.-W. Lee, S.-Y. Huang, A. A. Muhabie, J.-Y. Lai, D.-J. Lee and C.-C. Cheng, Highly stable photosensitive supramolecular micelles for tunable, efficient controlled drug release, *Eur. Polym. J.*, 2019, **110**, 403–412.

34 X. Chen, H. Gao, Z. Tang and G. Wang, Metal–organic framework-based phase change materials for thermal energy storage, *Cell Rep. Phys. Sci.*, 2020, **1**(10), 1–28.

35 P.-P. Zhao, C. Deng, Z.-Y. Zhao, S.-C. Huang, P. Lu and Y.-Z. Wang, Nanoflake-constructed supramolecular hierarchical porous microspheres for fire-safety and highly efficient thermal energy storage, *ACS Appl. Mater. Interfaces*, 2020, **12**(25), 28700–28710.

36 H. Zheng, C. Wang, Q. Liu, Z. Tian and X. Fan, Thermal performance of copper foam/paraffin composite phase change material, *Energy Convers. Manage.*, 2018, **157**, 372–381.

37 A. A. Muhabie, C.-C. Cheng, J.-J. Huang, Z.-S. Liao, S.-Y. Huang, C.-W. Chiu and D.-J. Lee, Non-covalently functionalized boron nitride mediated by a highly self-assembled supramolecular polymer, *Chem. Mater.*, 2017, **29**(19), 8513–8520.

38 M. Li, Q. Guo and S. Nutt, Carbon nanotube/paraffin/montmorillonite composite phase change material for thermal energy storage, *Sol. Energy*, 2017, **146**, 1–7.

39 H. Zhang, K. Yu, S. Gao, C. Wang, C. Wang, H. Wang and B. Zhou, Assembly of two-fold interpenetrated silver supramolecular coordination polymer using Keggin phosphotungstate template, *Inorg. Chem. Commun.*, 2014, **44**, 91–95.

40 R. Wen, M. Wu, J. Zhu, S. Zhu and W. Chen, Preparation and characteristic of Ag nanoparticle modified expanded graphite for enhancing paraffin phase change material properties, *Fullerenes, Nanotubes Carbon Nanostruct.*, 2022, **30**(10), 1046–1053.

41 H. Yuan, S. Liu, S. Hao, Z. Zhang, H. An, W. Tian, M. Chan and H. Bai, Fabrication and properties of nanoencapsulated stearic acid phase change materials with Ag shell for solar energy storage, *Sol. Energy Mater. Sol. Cells*, 2022, **239**, 111653.

42 T. Li, D. Wu, F. He and R. Wang, Experimental investigation on copper foam/hydrated salt composite phase change material for thermal energy storage, *Int. J. Heat Mass Transfer*, 2017, **115**, 148–157.

43 H. Yuan, H. Bai, H. Chen, Z. Zhang, H. An and W. Tian, Synthesis and properties of high thermal conductivity Ag shell-coated phase change materials, *Renewable Energy*, 2021, **179**, 395–405.

44 M. R. Yazdani, J. Etula, J. B. Zimmerman and A. Seppälä, Ionic cross-linked polyvinyl alcohol tunes vitrification and cold-crystallization of sugar alcohol for long-term thermal energy storage, *Green Chem.*, 2020, **22**(16), 5447–5462.